Low-Speed Sensorless Control of DFIG Generators Drive for Wind Turbines System

Badre Bossoufi[1] & Hala Alami Aroussi[1], ElMostafa Ziani[1], Ahmed Lagrioui[2], Aziz Derouich[3]

[1] Laboratory of Electrical Engineering and Maintenance, Higher School of Technology, EST-Oujda.
First Mohammed University, Morocco.
[2] Department of Electrical and Computer Engineering, Higher National School of Arts and Trades.
Moulay Ismail University Meknes, Morocco
[3] Department of Electrical and Computer Engineering, Higher School of Technology.
Sidi Mohamed Ben Abdellah University Fez, Morocco
Badre_isai@hotmail.com

Abstract: In this paper, we present a nonlinear robust control of active and reactive power by the use the PI regulators control (FOC) a Double-Fed Asynchronous Generator (DFIG) system incorporated in a wind-turbine. The power transfer between the stator and the network grid is carried out by acting on the rotor via a bidirectional signal converter. Initially, a control strategy of the MPPT-DFIG is presented. Thereafter, a new control technique for wind systems is presented. This control technique is based on an SVW placement control strategy. The overall stability of the system is shown using SVW block. The performance and robustness are analyzed and compared by simulation based Matlab / Simulink software.
Keywords: DFIG-Generator, Rotor Control, Matlab/Simulink, Wind-Turbine, MPPT Control, SVW.

1. Introduction

Recently, the wind energy has become a viable solution for the production of energy, in addition to other renewable energy sources. While the majority of wind turbines are fixed speed, the number of variable speed wind turbines is increasing [1-2]. *The* Doubly-Fed Asynchronous Generator (*DFIG*) with FOC control is a machine that has excellent performance and is commonly used in the wind turbine industry. There are many reasons for using an Doubly-Fed Asynchronous Generator (DFIG) for wind turbine a variable speed , such as reducing efforts on mechanical parts, noise reduction and the possibility of control of active power and reactive.

The wind system using DFIG generator and a "back-to-back" converter that connects the rotor of the generator and the network has many advantages. One advantage of this structure is that the power converters used are dimensioned to pass a fraction of the total system power [3-4]. This allows reducing losses in the power electronics components. The performances and power generation depends not only on the DFIG generator, but also the manner in which the two parts of "back-to-back" converter are controlled.

The power converter machine side is called "Rotor Side Converter RSC" (PWM Inverter 1) and the converter Grid-side power is called "Grid Side Converter GSC" (PWM Inverter 2). The RSC converter controls the active power and reactive power produced by the machine. As the GSC converter, it controls the DC bus voltage and power factor network side.

According to the application, consider several algorithms of control can be used such as the current control algorithms, of active or reactive power, speed, position...etc. the structure as of the these control algorithms generally comprises an internal loop of regulation of the current. Finally is often most difficult to implement because it generally constitutes the most complex part of the control algorithm. The other control loops are relatively much simpler to implement. This is why, within the framework of this work, one will particularly be interested in the current control technique implementation of the electric machines "the PI Regulators Control (FOC)".

In this paper, we present a technique to control two power converters which is based on the FOC control. We analyze their dynamic performances by simulations in Matlab/Simulink environment. We start by modeling of the wind turbine, and then a tracking technique operating point at maximum power point tracking (MPPT) will be presented. Thereafter, we present a model of the DFIG in the d-q reference, and the general principle of control of both power converters which is based on FOC-SVW technique [5-6-7].

Considering the complexity of the diversity of the electric control devices of the machines, it is difficult to define with universal manner a general structure for such systems. However, by having a reflexion compared to the elements most commonly encountered in these systems, it is possible to define a general structure of an electric control device of machines which is show in *Fig.1*:
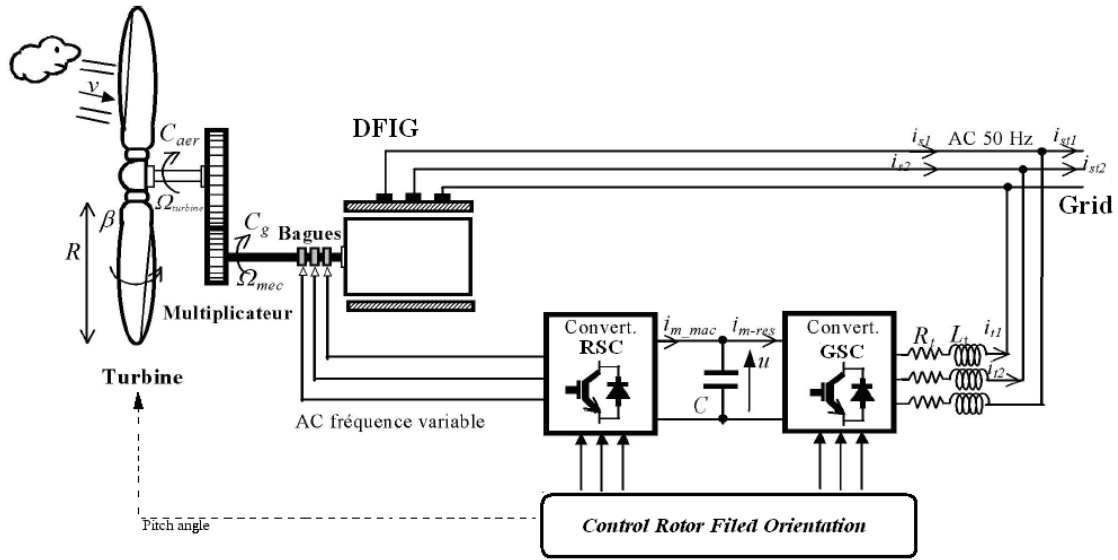
Badre Bossoufi, Hala Alami Aroussi,
ElMostafa Ziani, Ahmed Lagrioui, Aziz Derouich

Fig.1: Architecture of the Control

2. Modelling of the Wind-Turbine

By applying the theory of momentum and Bernoulli's theorem, we can determine the incident power (theoretical power) due to wind [5]:

$$P_{incident} = \frac{1}{2}.\rho.S.v^3 \qquad (1)$$

S : the area swept by the pales of the turbine $[m^2]$
ρ : the density of the air ($\rho = 1.225 kg / m^3$ at atmospheric pressure).
v : wind speed $[m/s]$

In wind energy system due to various losses, available on the power extracted from the turbine rotor, is lower than the incident power. The power extracted is expressed by [9]:

$$P_{extracted} = \frac{1}{2}.\rho.S.C_p(\lambda,\beta).v^3 \qquad (2)$$

Cp (λ, β) is called the power coefficient, which expresses the aerodynamic efficiency of the turbine. It depends on the ratio λ, which represents the ratio between the speed at the end of the blades and the wind speed and the angle of orientation of the blades β. The ratio λ can be expressed by the following relation [9]:

$$\lambda = \frac{\Omega_t.R}{v} \qquad (3)$$

The maximum power coefficient Cp was determined by Albert Betz (1920) as follows:

$$C_p^{max}(\lambda,\beta) = \frac{16}{27} \approx 0.593 \qquad (4)$$

The power factor is intrinsic to the constitution of the wind-turbine and depends on the profiles of the blades. We can model the power coefficient with a single equation that depends on the speed ratio λ and pitch angle β for the blade [9]:

$$C_p(\lambda,\beta) = c_1.\left(c_2.\frac{1}{A} - c_3.\beta - c_4 \right).e^{-c_5\frac{1}{A}} + c_6.\lambda \qquad (5)$$

$c_1 = 0.5872$, $c_2 = 116$, $c_3 = 0.4$, $c_4 = 5$, $c_5 = 21$, $c_6 = 0.0085$
The six coefficients c_1, c_2, c_3, c_4, c_5 are modified for maximum Cp equal to 0.498 for $\beta = 0°$.
With A which depends on λ and β:

$$\frac{1}{A} = \frac{1}{\lambda + 0.08.\beta} - \frac{0.035}{1 + \beta^3} \qquad (6)$$

The *Fig.2* shows the curves of the power coefficient as a function of λ for different values of β. A coefficient of maximum power of 0.498 is obtained for a speed ratio λ which is 8 (λ_{opt}). Fixing β and λ respectively to their optimal values, the wind system provides optimal power [10-11].
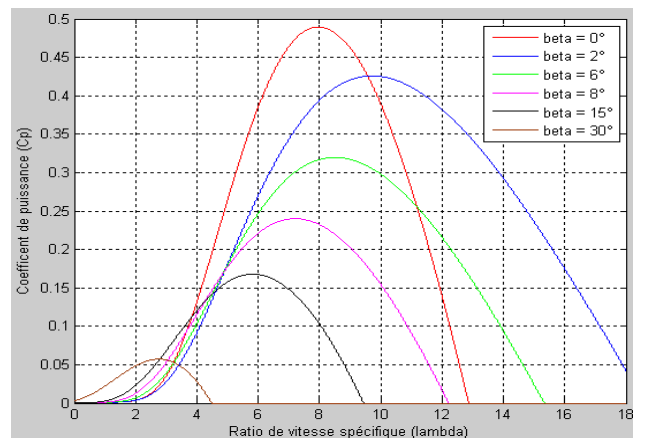

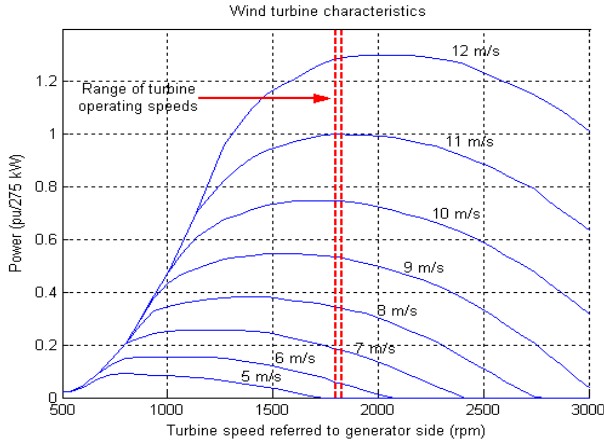Fig.2: Power coefficient as a function of λ and β

Fig.3: Wind-turbine DFIG characteristics

The aerodynamic torque on the slow axis can be expressed by Equation 7: [12-13]

$$C_{al} = \frac{P_{eol}}{\Omega_t} = \frac{1}{2}.\rho.S.C_p(\lambda,\beta).v^3.\frac{1}{\Omega_t} \qquad (7)$$

Ω_t : Rotational speed of the turbine
C_{al} : Torque on the slow axis (turbine side)

The mechanical speed is related to the speed of rotation of the turbine by the coefficient of the multiplier. The torque on the slow axis is connected to the torque on the fast axis (generator side) by the multiplier coefficient.

The total inertia J is formed of the reduced inertia of the turbine and the fast axis of the inertia J of the generator g [12]:

$$J = \frac{J_{tur}}{G^2} + J_g \qquad (8)$$

J_{tur} : turbine inertia
J_g : inertia of the generator.

To determine the evolution of the mechanical speed from C_{mec} total torque applied to the rotor of the DFIG, we apply the fundamental equation of dynamics:

$$J\frac{d\Omega_{mec}}{dt} = C_{mec} = C_{ar} - C_{em} - f.\Omega_{mec} \qquad (9)$$

Ω_{mec} : Mechanical speed of DFIG
C_{ar} : Aerodynamic torque on the fast axis of the turbine
C_{em} : Electromagnetic torque
f : Friction.

The above equations are used to prepare the block diagram of the model of turbine (Fig.4).
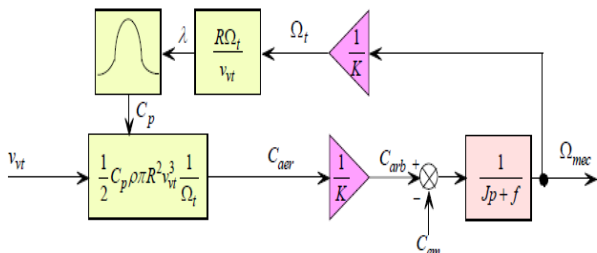

Fig.4: Wind-turbine model

3. Extraction of Maximum Power

In order to capture the maximum power of the incident energy of the wind-turbine, must continuously adjust the rotational speed of the wind turbine. The optimal mechanical turbine speed corresponds has λopt and β = 0°. The speed of the DFIG is used as a reference value for a controller proportional-integral type (PI phase advance). The latter determines the control set point which is the electromagnetic torque that should be applied to the machine to run the generator at its optimal speed.

The torque thus determined by the controller is used as a reference torque of the turbine model (Fig.5). The system of variation of the angle of orientation of the blades (variation of the angle of incidence) to change the ratio between the lift and drag. To extract the maximum power (and maintain constant), the adjusted angle of incidence of the blades to the wind speed [14-15].

The "Pitch Control" is a technique that mechanically adjusts the blade pitch angle to shift the curve of the power coefficient of the turbine.

However, it is quite expensive and is generally used for wind turbines and high average power. For our model, the "Stall Control" technique, which is a passive technique that allows a natural aerodynamic stall (loss of lift when the wind speed becomes more important). La régulation de la vitesse de rotation de l'angle de pas des pales de la turbine se produit lorsque la vitesse de la génératrice est supérieure à 30% de sa vitesse nominale. Otherwise, β is zero. The synthesis of the PI controller requires knowledge of the transfer function of our system. This is especially difficult because of the power coefficient. A simple proportional correction (P) is obtained after testing. Note that β may vary from 0 ° to 90 ° characterized by saturation.
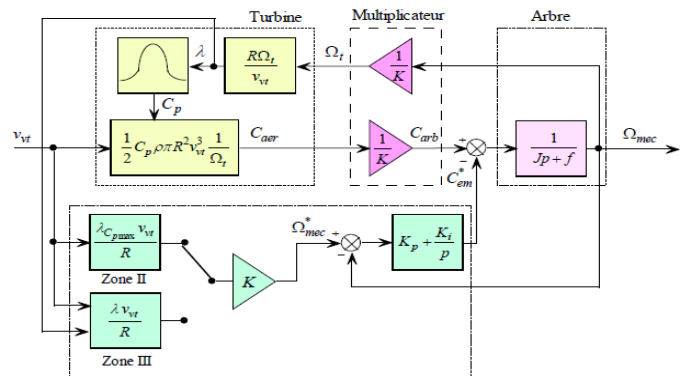

Fig.5: Block diagram with control of the speed

4. Equivalent model of FOC DFIG-Generator

4.1. Control Architecture

The Figure 6 shows the architecture of a control system applied FOC based DFIG has:

Badre Bossoufi, Hala Alami Aroussi,
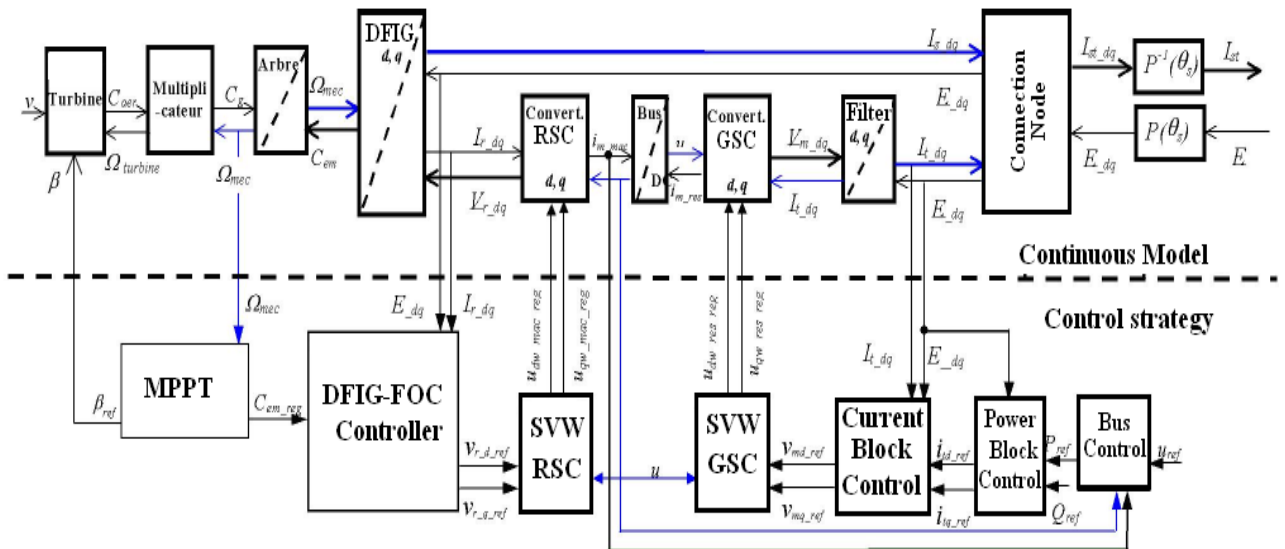ElMostafa Ziani, Ahmed Lagrioui, Aziz Derouich

Fig.6: Conversion chain based on the machine DFIG

The controller can be divided into two parts. The RSC Converter (SVW-RSC) controls the flux and the speed of the generator DFIG. The GSC Converter (SVW-GSC) controls the DC bus voltage and active and reactive power exchanged with the network and establishes the frequency of the current distribution network.
The control of DFIG is based on three features:

✓ The extraction algorithm of maximum power of MPPT;
✓ The vector control of DFIG;
✓ RSC Control converter.

4.2. FOC Controller of DFIG.
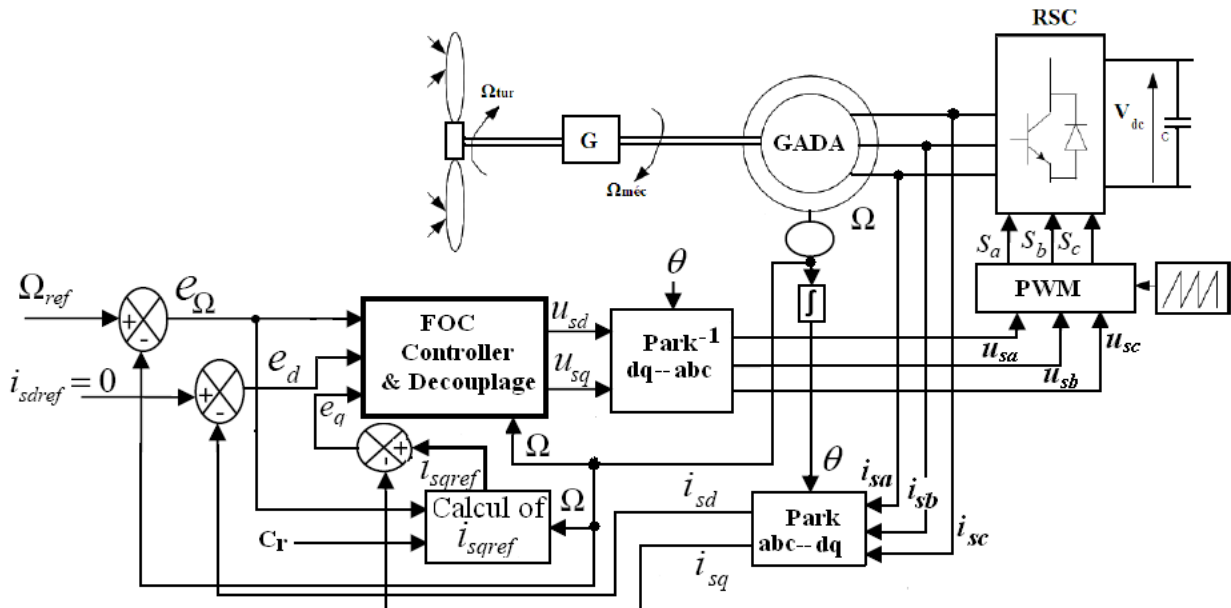
Fig.7: Simulation scheme of FOC Control applied for DFIG-wind-turbine

"The flux control oriented" applied to the electric motors is used to obtain the desired operating mode by optimally positioning a current flux and the resulting vectors.
Many variants of this control principle have been presented in the literature which may have classified according to the orientation of the reference frame (d-q) on:

✓ The rotor flux,

✓ The stator flux,
✓ The air gap flux.
Following the determination of the position of the stream;
✓ By direct measurement or observation of the flux vector (modulus, phase).
✓ Indirect by control the frequency of slippage.
In this work, we develop the vector generator control DFIG with orientation mark (d-q) following the rotor flux.

The latter is divided into 3 parts:
- ✓ Flux control,
- ✓ The control of stator currents,
- ✓ Decoupling or compensation.

4.3. DFIG Model System

The Power equations in the d-q reference DFIG can be written [17-18]:

$$
\begin{cases}
\dfrac{d\Phi_{sd}}{dt} = v_{sd} - R_s.i_{sd} + \Phi_{sq}\omega_s \\[2mm]
\dfrac{d\Phi_{sq}}{dt} = v_{sq} - R_s.i_{sq} - \Phi_{sd}\omega_s \\[2mm]
\dfrac{d\Phi_{rd}}{dt} = v_{rd} - R_r.i_{rd} + \Phi_{rq}\omega_r \\[2mm]
\dfrac{d\Phi_{rq}}{dt} = v_{rq} - R_r.i_{rq} - \Phi_{rd}\omega_r
\end{cases}
\tag{10}
$$

By directing a flux of the model obtained from the DFIG is simplified and the resulting control of the device is also. The vector control of this machine was designed by moving the marker to the Park along the axis q is constantly zero stator flux: $\Phi_{sq} = 0$

$$
\begin{cases}
\dfrac{d\Phi_{sd}}{dt} = v_{sd} - R_s.i_{sd} \\[2mm]
v_{sq} = R_s.i_{sq} + \Phi_{sd}.\omega_s \\[2mm]
\dfrac{d\Phi_{rd}}{dt} = v_{rd} - R_r.i_{rd} + \Phi_{rq}\omega_r \\[2mm]
\dfrac{d\Phi_{rq}}{dt} = v_{rq} - R_r.i_{rq} + \Phi_{rd}\omega_r
\end{cases}
\tag{11}
$$

From the equations of direct and quadrature components of the stator flux, the following expressions of stator currents are obtained:

$$
i_{sq} = -\frac{M}{L_s}.i_{rq}
\tag{12}
$$

$$
i_{sd} = \frac{\Phi_{sd} - M.i_{rd}}{L_s}
\tag{13}
$$

These stator currents are replaced in equations direct and quadrature components of the rotor flux:

$$
\Phi_{rd} = (L_r - \frac{M^2}{L_s}).i_{rd} + \frac{M}{L_s}.\Phi_{sd} = L_r.\sigma.i_{rd} + \frac{M}{L_s}.\Phi_{sd}
\tag{14}
$$

$$
\Phi_{rq} = L_r.i_{rq} - \frac{M^2}{L_s}.i_{rq} = L_r.\sigma.i_{rq}
\tag{15}
$$

σ is the dispersion coefficient between the windings and q:

$$
\sigma = 1 - \frac{M^2}{L_s.L_r}
$$

We are obtained:

$$
\begin{cases}
v_{sd} = \dfrac{R_s}{L_s}.\Phi_{sd} - \dfrac{R_s}{L_s}.M.i_{rd} + \dfrac{d\Phi_{sd}}{dt} \\[3mm]
v_{sq} = -\dfrac{R_s}{L_s}.M.i_{rq} + \omega_s.\Phi_{sd} \\[3mm]
v_{rd} = R_r.i_{rd} + L_r.\sigma.\dfrac{di_{rd}}{dt} + \dfrac{M}{L_s}.\dfrac{d\Phi_{sd}}{dt} - L_r.\omega_r.\sigma.i_{rq} \\[3mm]
v_{rq} = R_r.i_{rq} + L_r.\sigma.\dfrac{di_{rq}}{dt} + L_r.\omega_r.\sigma.i_{rd} + \omega_r.\dfrac{M}{L_s}.\Phi_{sd}
\end{cases}
\tag{16}
$$

From equations 3 and 4 of the 16 system, we get:

$$
\frac{di_{rd}}{dt} = \frac{1}{L_r.\sigma}\left[v_{rd} - R_r.i_{rd} + L_r.\omega_r.\sigma.i_{rq} - \frac{M}{L_s}.\frac{d\Phi_{sd}}{dt} \right]
\tag{17}
$$

$$
\frac{di_{rq}}{dt} = \frac{1}{L_r.\sigma}\left[v_{rq} - R_r.i_{rq} + L_r.\omega_r.\sigma.i_{rd} - \omega_r.\frac{M}{L_s}.\Phi_{sd} \right]
\tag{18}
$$

Noting the following f.e.m:

$$
\begin{cases}
e_d = L_r.\omega_r.\sigma.i_{rq} + \dfrac{M}{L_s}.\dfrac{d\Phi_{sd}}{dt} \\[3mm]
e_\Phi = \omega_r.\dfrac{M}{L_s}.\Phi_{sd} \\[3mm]
e_q = L_r.\omega_r.\sigma.i_{rd}
\end{cases}
\tag{19}
$$

We are obtained:

$$
\frac{di_{rd}}{dt} = \frac{1}{L_r.\sigma}\left[v_{rd} - R_r.i_{rd} - e_d \right]
\tag{20}
$$

$$
\frac{di_{rq}}{dt} = \frac{1}{L_r.\sigma}\left[v_{rd} - R_r.i_{rq} - e_q - e_\Phi \right]
\tag{21}
$$

The torque is expressed as:

$$
C_{em} = p.(\Phi_{sd}.i_{rq} - \Phi_{sq}.i_{rd})
\tag{22}
$$

With an orientation of the stator flux as $\Phi_{sq}=0$, we are obtained:
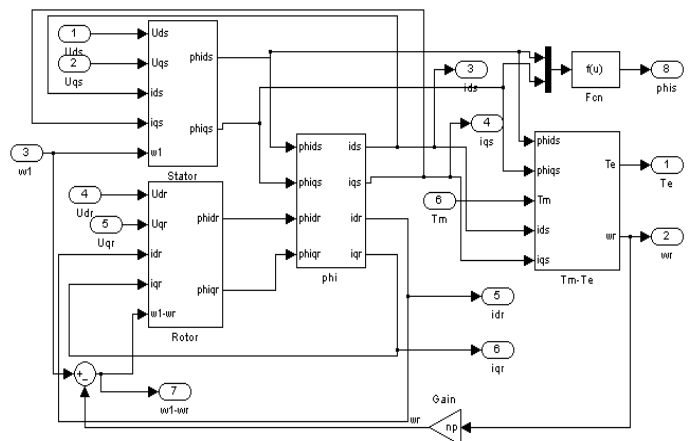
$$
C_{em} = p.\Phi_{sd}.i_{rq}
\tag{23}
$$

Fig.8: DFIG Model for wind-turbine

Badre Bossoufi, Hala Alami Aroussi,
ElMostafa Ziani, Ahmed Lagrioui, Aziz Derouich

4.4. Flux Control Algorithm

4.4.1. Principle

The knowledge of the stator flux and its use in the control of DFIG-Generator will affect the overall behavior of the wind generator, especially at the onset of a voltage dip. In this section, we present two techniques for obtaining an estimate of the direct component of the stator flux and various control strategies:

> ➢ A synchronous approach based on flux control in open loop, it is an approach which assumes that the flux is determined by the grid network.
> ➢ An asynchronous approach based on flow control closed-loop, when the voltage is varied. This estimate, a flux control is essential.

4.4.2. Flux Control Estimator

From equation 16 it can be determined by a dynamic estimate of the d-axis stator flux:

$$\hat{\Phi}_{sd} = \frac{1}{1+\dfrac{L_s}{R_s}.s}\left[\frac{L_s}{R_s}v_{sd} + M.i_{rd}\right] \qquad (24)$$

La composante du flux Φ_{sd} est estimée alors par l'équation suivante :

$$\Phi_{sd} = L_s.i_{sd} + M.i_{rd} \qquad (25)$$

4.5. PI regulators control structure

This part is focuses on setting by Space Vector Modulation, d and q components of vector current stator of the *DFIG-generator* in the *d-q* rotating coordinate system. The choice of this coordinate system for the *PI* controllers setting completion is because the direct and transverse components of the vector current stator in this case are continuous magnitudes in steady state. The module of the vector stator can be adjusted with high accuracy because the integral *PI* regulator cancels the error in steady state. As the phase of the vector current stator, it is taxed correctly via coordinate transformations as the transformations of Park and Park opposite.

The output quantities of an order based on *PI* regulators to control the current tensions are obtained at the terminals of the machine. These tensions are then reconstructed using the Pulse Width Modulation technique (*SVM*).

This technique considers the overall *SVM* phase system. It generates the reference vector voltage in the average values during the sampling progress, and this through the calculation in times domain of active vectors which define the area in which is the reference voltage vector [5-8]. The goal of *SVM* is control impose order, at each period of hash, an average voltage across each phase of the load equal to its reference voltage. To do this, the reports generated at each cyclical period hashing must verify the relation (1) to ensure the realization of this relationship for the two variants of *SVM*.

$$\begin{bmatrix} V_{sa}(t) \\ V_{sb}(t) \\ V_{sc}(t) \end{bmatrix} = \begin{bmatrix} V_{an}(t) \\ V_{bn}(t) \\ V_{cn}(t) \end{bmatrix} = \frac{E}{3}\begin{bmatrix} 2 & -1 & -1 \\ -1 & 2 & -1 \\ -1 & -1 & 2 \end{bmatrix}\begin{bmatrix} S_a(t) \\ S_b(t) \\ S_c(t) \end{bmatrix} \qquad (26)$$

The reference voltages $V_{10}(t)$, $V_{20}(t)$ and $V_{30}(t)$ are compared with the triangular carrier signal is shown in *Fig.7*:
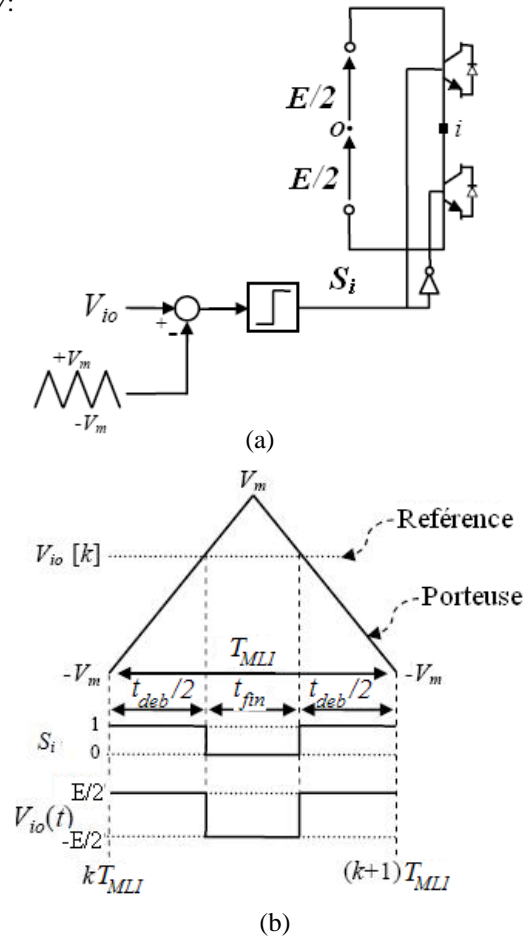

Fig.9: (a) block diagram of the PWM controlled arm i of the inverter voltage (b) PWM function principle.

In Fig.9, the t_{on} and t_{off} time correspond to the taken time by the control signal S_i respectively at logic high and low logic. T_{PWM} is the period of the carrier. V_{io} (k) is the voltage reference of the ith arm during the kth hash period. The control signal S_i is arm of the inverter voltage it high logic when the reference voltage exceeds the carrier and low logic otherwise. The voltage $V_i(t)$ is equal to $+E/2$ if the reference voltage is greater than the carrier and $E/2$ otherwise.

The Fig.10 presents a description of the switching control signals S_a, S_b and S_c corresponding to a vector *PWM*.
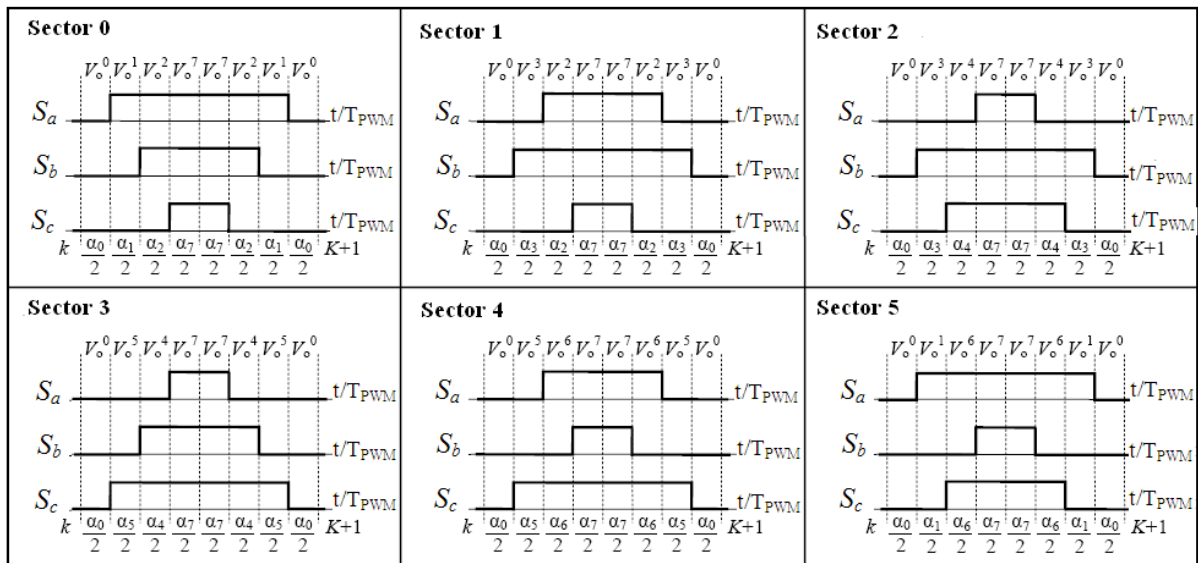
Fig.10: Switching description of the SVM vector.

5. Simulation results

The overall model of the wind system was simulated in Matlab/ Simulink/SimPowerSystems environment. The model includes: wind turbine, Doubly-Fed Asynchronous Generator (DFIG), two power converters that connect the rotor to the network (Figure 11).
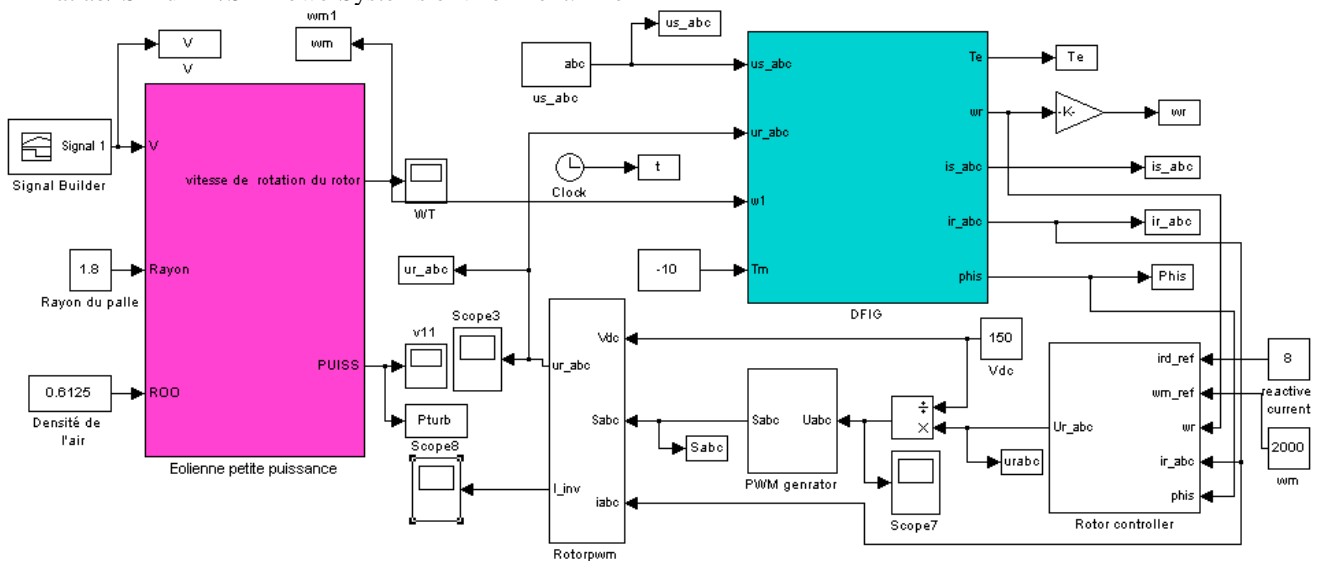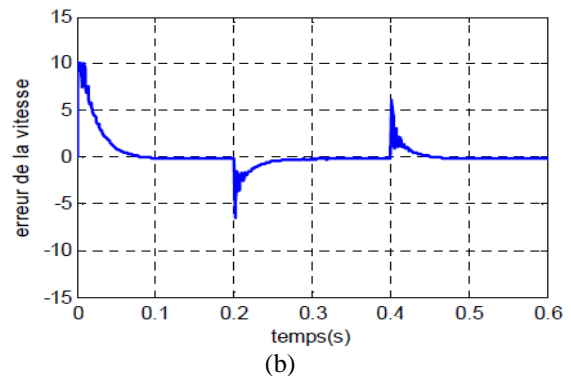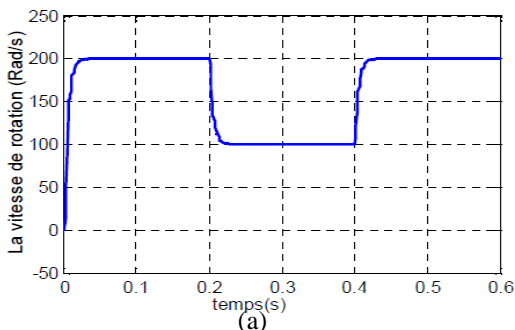

Fig.11: Simulation scheme of FOC Control applied for DFIG-wind-turbine
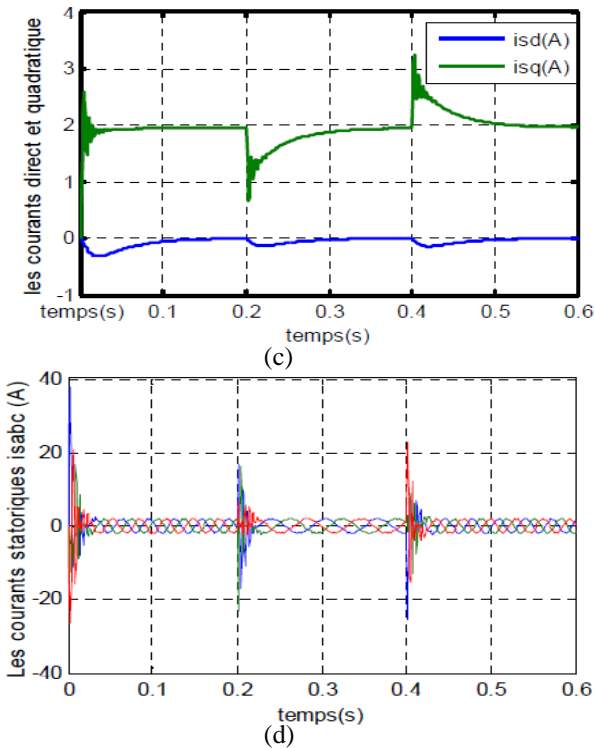
5.1. DFIG performances

➢ **Follow of the trajectory**

(a)

(b)

Badre Bossoufi, Hala Alami Aroussi,
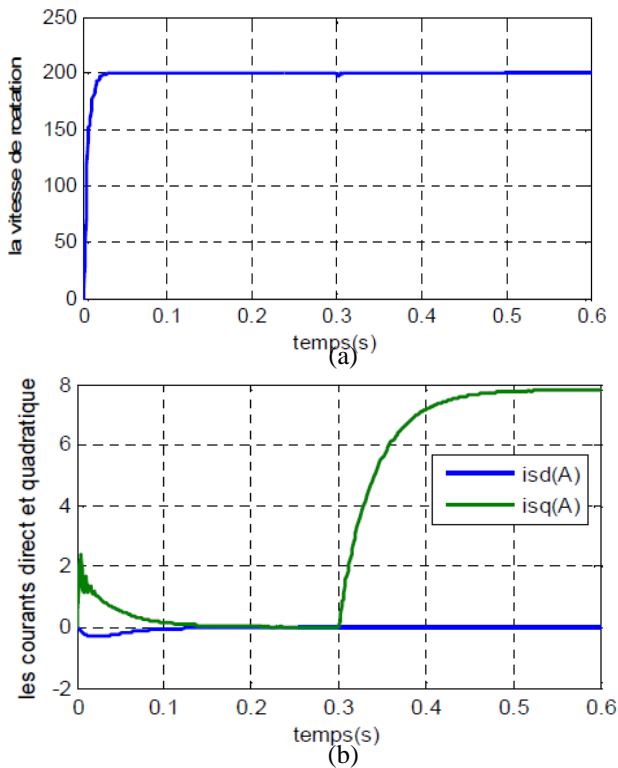ElMostafa Ziani, Ahmed Lagrioui, Aziz Derouich

(c)

(c)

Fig.13: Test performance of the FOC controller for
rejecting disturbance torque load applied at t = 0.3s.
(a)Speed response trajectory (b) d-q axis current without
uncertainties (c) Electromagnetic Torque

➢ **Parametric uncertainties**

(a)

(d)

Fig.12: Test performance of the FOC controller for
trajectory tracking, (a) Speed response trajectory (b)
Error Speed response (c) d-q axis current without
uncertainties (d) abc axis current

➢ **Disturbance rejection**

(a)

(b)

(b)

(c)
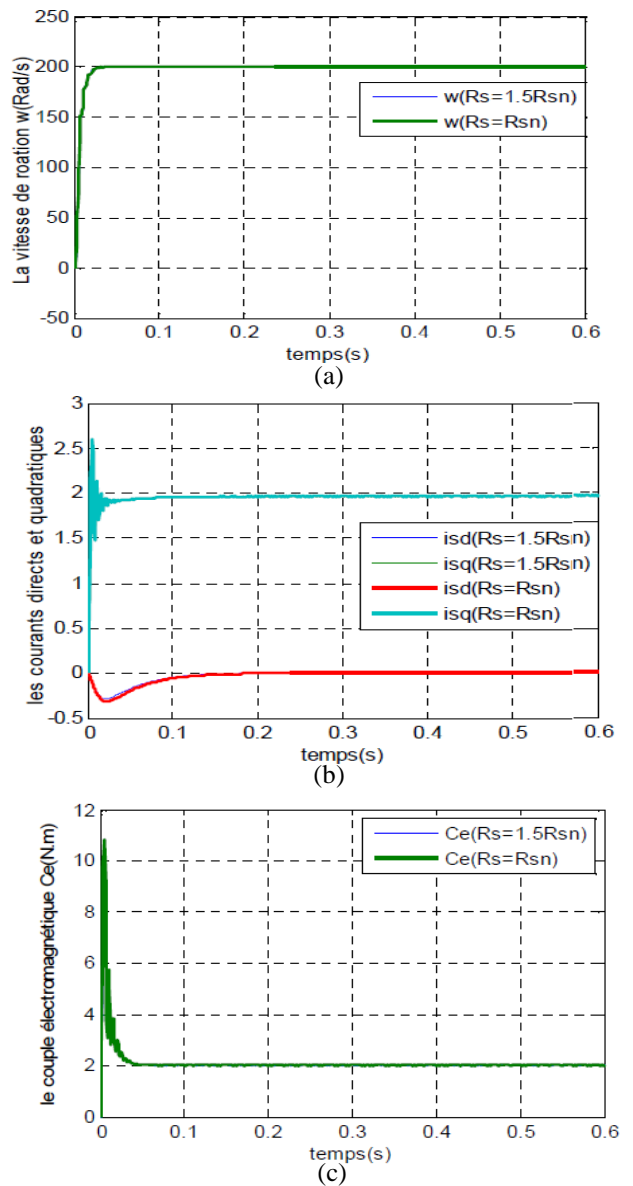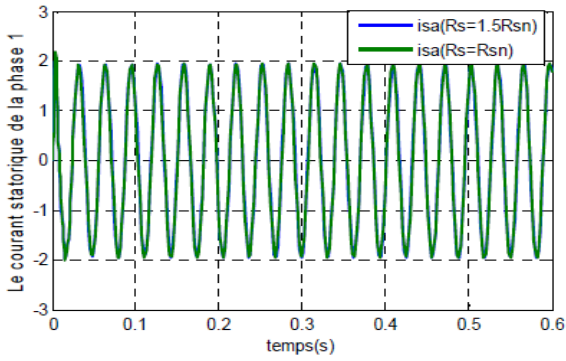
(d)

Fig.14: Test performance of the FOC controller following
a change in Rs. (a) Speed response trajectory (b) d-q axis
current without uncertainties (c) Electromagnetic Torque
(d) current isa

5.2. Wind-turbine performances

Using the reduced model, we applied a profile closer
to the evolution of the real wind was filtered to suit the
slow dynamics of the system studied random wind. The
objective is to see the degree of continuing point of
maximum power and efficiency of the speed control
provided by the FOC controller. The *Fig.15* shows the
wind profile filtered and applied to the system in this
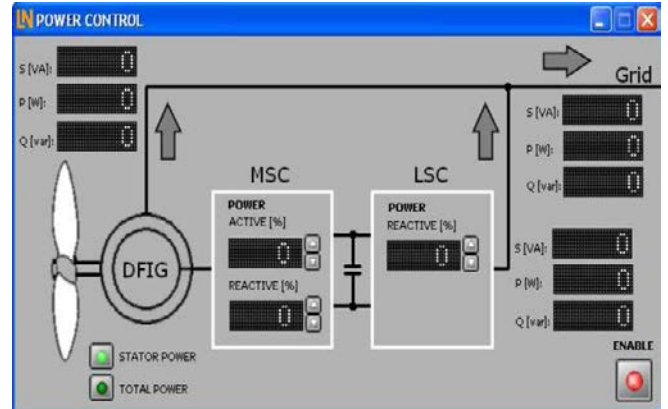case.

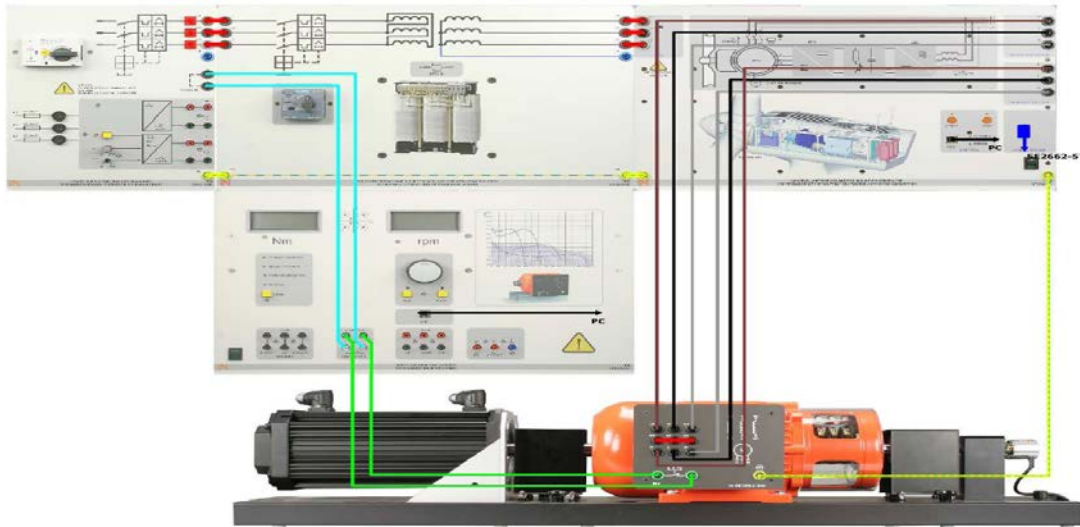Fig.15: DFIG-Generator with wind turbine interface

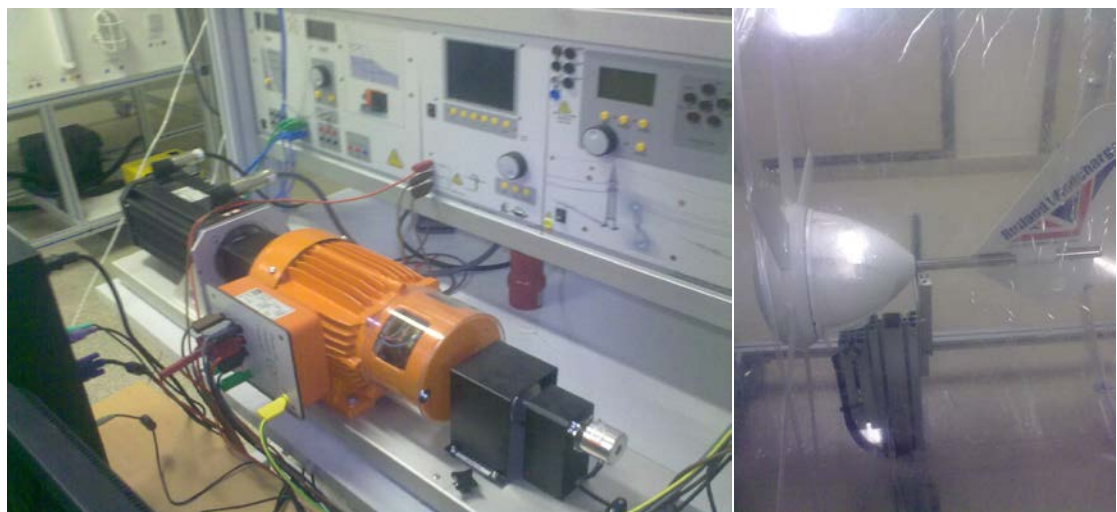Fig.16: Benchmark of Wind Turbine System

Fig.17: Experimental Benchmark of Wind Turbine System

The *Fig.18* shows the wind profile filtered and applied to the system in this case.
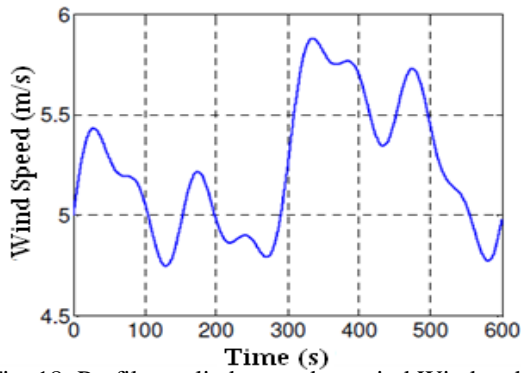

Fig. 18: Profile applied to random wind Wind-turbine.

The figure 19 shows the results obtained for this application, where the following observations can be distinguished:

➢ The specific speed λ and the power coefficient C_p does not change a lot of values, they are almost equal to their optimal values references 9 and 0.4999 successively;

➢ The wind power captured follows its optimal reference and has the same shape as the wind profile applied, this rate is also consistent with the wind torque side of the MADA;

➢ The speed of the DFIG is the image of wind causing the wind, it properly follows its reference;

➢ The shapes of the electromagnetic torque of the DFIG and its reference, are virtually identical, but different from the shape of the profile of the wind speed due to the dynamic torque due to inertia;

➢ The phase shift between the voltage 180˚ and the stator current phase reflects a production of active power only to the stator as illustrated in figure powers;

➢ The shape of the components of the stator flux orientation shows a good flow to ensure vector control well decoupled from the DFIG.

Badre Bossoufi, Hala Alami Aroussi,
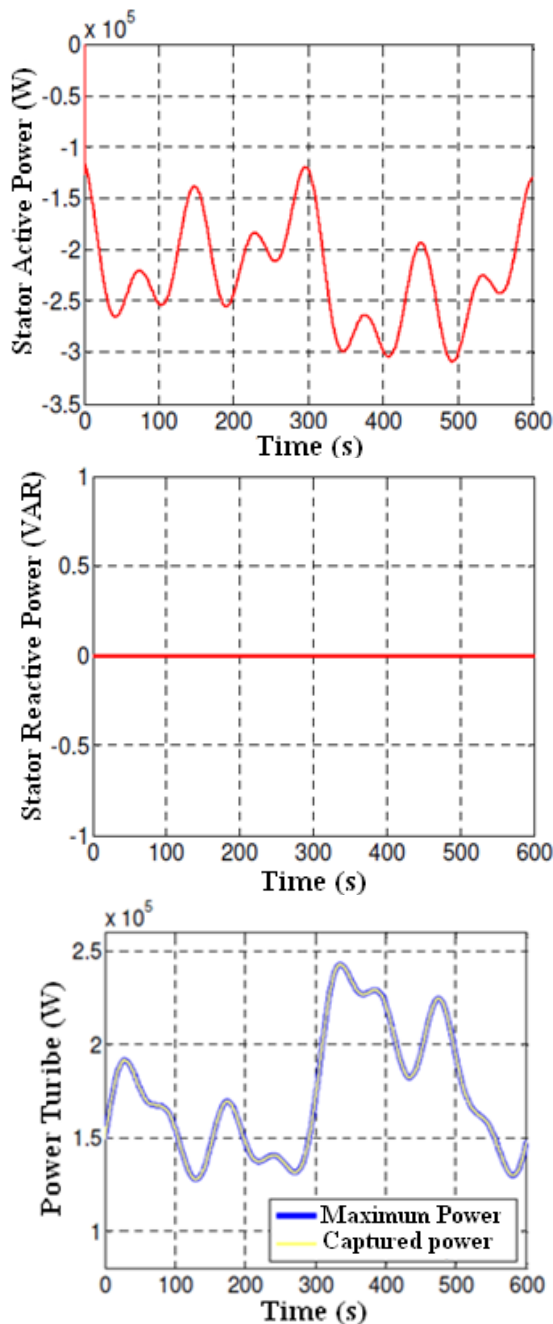ElMostafa Ziani, Ahmed Lagrioui, Aziz Derouich
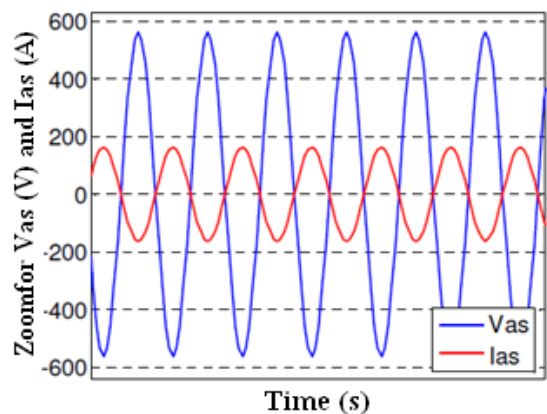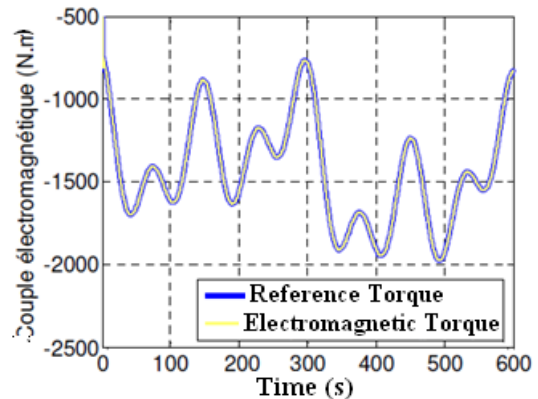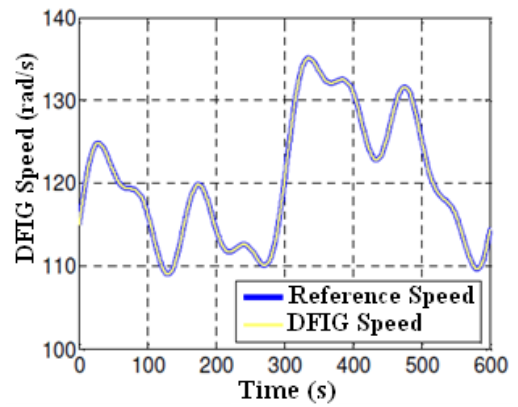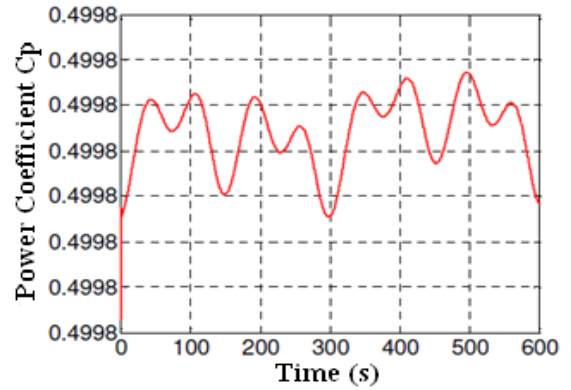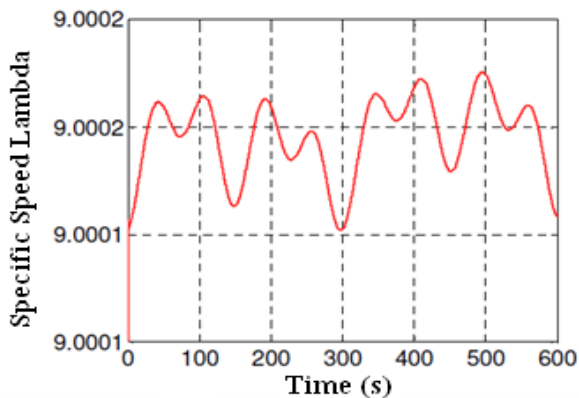
Fig.19: The Simulation results of the asynchronous wind generator dual power and stator flux oriented, with a Backstepping controller (Case scale model of the DFIG and profile of random wind).

6. Conclusion

This work has been devoted to modeling, simulation and analysis of a wind turbine operating at variable speed. A stable operation of the wind energy system is obtained with the application of nonlinear Backstepping Adaptive control. The overall operation of the wind turbine and its control system were illustrated by responses to transient and permanent control systems.

Generator supplied power to the network with an active power whatever the mode of operation. The wind generator has been tested and modeled with a variable speed operation for a power of 200 kW. Simulation

results show that the proposed wind system and is feasible and has many advantages.

REFERENCES

[1] T. Ackermann and Soder, L. « An Overview of Wind Energy-Status 2002 ». Renewable and Sustainable Energy Reviews 6(1-2), 67-127 (2002).

[2] T. Burton, D. Sharpe, N. Jenkins and E. Bossanyi, *Wind Energy Handbook*. John Wiley&Sons, Ltd, 2001.

[3] W. L. Kling and J. G. Slootweg, « Wind Turbines as Power Plants». in Proceeding of the IEEE/Cigré workshop on Wind Power and the impacts on Power Systems, 17-18 June 2002, Oslo, Norway.

[4] D. Seyoum, C. Grantham, «Terminal Voltage Control of a Wind Turbine Driven Isolated Induction Generator using Stator Oriented Field Control». IEEE Transactions on Industry Applications, pp. 846-852, September 2003.

[5] A. DAVIGNY, *Participation aux services système de fermes éoliennes à vitesse variable intégrant un stockage inertiel d'énergie*, Thèse de Doctorat, USTL Lille (France), 2007.

[6] K. GHEDAMSI, *Contribution à la modélisation et la commande d'un convertisseur direct de fréquence. Application à la conduite de la machine asynchrone*, Thèse de Doctorat, ENP Alger (Algérie), 2008.

[7] Bossoufi, B., Karim, M., Lagrioui, A. "Matlab & Simulink Simulation with FPGA-Based Implementation adaptative and not adaptative backstepping nonlinear Control of a Permanent Magnet Synchronous Machine Drive" *Wseas Transactions on Systems and Control*, Vol.9 No.1, pp 92-103, March 2014.

[8] Bossoufi, B., Karim, M. Ionita, S., Lagrioui, A.,"Indirect Sliding Mode Control of a Permanent Magnet Synchronous Machine: FPGA-Based Implementation with Matlab & Simulink Simulation" *Journal of Theoretical and Applied Information Technology JATIT*, Vol. 29 No.1, pp32-42, 15 July 2011.

[9] Bossoufi, B., Karim, M. Ionita, S., Lagrioui, A. "The Optimal Direct Torque Control of a PMSM drive: FPGA-Based Implementation with Matlab & Simulink Simulation" *Journal of Theoretical and Applied Information Technology JATIT*, Vol. 28 No.2, pp63-72, 30 June 2011.

[10] Bossoufi, B., Karim, M. Ionita, S., Lagrioui, A. "DTC CONTROL BASED ARTIFICIAL NEURAL NETWORK FOR HIGH PERFORMANCE PMSM DRIVE" *Journal of Theoretical and Applied Information Technology JATIT*, Vol.33 No.2, pp165-176, 30 November 2011.

[11] Bossoufi, B., Karim, M. Ionita, S., Lagrioui, A. "Nonlinear Non Adaptive Backstepping with Sliding-Mode Torque Control Approach for PMSM

Motor" *Journal of Journal of Electrical Systems JES*, Vol.8 No.2, pp236-248, June 2012.

[12] B.Bossoufi, M.Karim, A.Lagrioui, M.Taoussi, M.L.EL Hafyani "Backstepping control of DFIG Generators for Wide-Range Variable-Speed Wind Turbines " *IJAAC International Journal of Automation and Control* , pp 122-140, Vol.8 No.2, July 2014.

[13] B.Bossoufi, M.Karim, S.Ionita, A.Lagrioui, "Performance Analysis of Direct Torque Control (DTC) for Synchronous Machine Permanent Magnet (PMSM)" 2010 IEEE 16th International Symposium for Design and Technology of Electronics Packages, IEEE-SIITME'2010, art. No. 5649125, pp.237-242. Pitesti, Romania.

[14] Bossoufi, B., Karim, M. Ionita, S., Lagrioui, A., (2012b) "Low-Speed Sensorless Control of PMSM Motor drive Using a NONLINEAR Approach BACKSTEPPING Control: FPGA-Based Implementation" Journal of Theoretical and Applied Information Technology JATIT, 29 February, Vol. 36 No.1, pp154-166.

[15] X. YU, K. STRUNZ, « Combined long-term and shortterm access storage for sustainable energy system », 2004 IEEE Power Engineering Society General Meeting, vol.2, pp.1946-1951, 10 June 2004.

[16] S. E. Ben Elghali, « Modélisation et Commande d'une hydrolienne Equipée d'une génératrice Asynchrone Double Alimentation », JGGE'08, 16-17 Décembre 2008, Lyon (France).S

[17] E. AIMANI, *Modélisation de différentes technologies d'éoliennes intégrées dans un réseau de moyenne tension*, Thèse de Doctorat, École Centrale de Lille (France), 2004.

[18] X. YAO, C. YI, D. YING, J. GUO and L. YANG, « The grid-side PWM Converter of the Wind Power Generation System Based on Fuzzy Sliding Mode Control », Advanced Intelligent Mechatronics, IEEE 2008, Xian (Chine).

[19] A. BOYETTE, « Contrôle-commande d'un générateur asynchrone à double alimentation avec système de stockage pour la production éolienne », Thèse de Doctorat, Nancy (France), 2006.